ONCOIMMUNOLOGY
2020, VOL. 9, NO. 1, 1–11
https://doi.org/10.1080/2162402X.2020.1836768

Taylor & Francis
Taylor & Francis Group

ORIGINAL RESEARCH

Reduction of CD11b$^+$ myeloid suppressive cells augments anti-neuroblastoma immune response induced by the anti-GD$_2$ antibody ch14.18/CHO

Nikolai Siebert, Maxi Zumpe, Leon von Lojewski, Sascha Troschke-Meurer, Madlen Marx, and Holger N. Lode

Department of Pediatric Oncology and Hematology, University Medicine Greifswald, Greifswald, Germany

ABSTRACT

Neuroblastoma (NB) still remains a major challenge in pediatric oncology. We recently showed CD11b$^+$-dependent upregulation of the PD-1/PD-L1 checkpoint on NB cells treated with the chimeric anti-GD$_2$ antibody (Ab) ch14.18/CHO. Here, we report effects of reduction of CD11b$^+$ myeloid suppressive cells on ch14.18/CHO immunotherapy against NB. Flow cytometry, immunohistochemistry and RT-PCR were used to assess tumor infiltrating leukocytes and expression of myeloid suppressive cell-associated genes. XTT assay was used to show impact of 5-FU on tumor and effector cells. Antitumor effects of the combined treatment with ch14.18/CHO and reduction of myeloid suppressive cells were evaluated in a syngeneic NB mouse model. Tumor tissue of untreated mice showed a strong infiltration by CD11b$^+$ cells (53% of all tumor infiltrating leukocytes). RT-PCR analysis of tumors revealed strong expression of the myeloid suppressive cell-associated genes analyzed with the strongest induction of M-CSFr, CCL2, IL-1β, IL-4, IL-6 r, IL-8, Arg1, and NOS2. Compared to controls, application of anti-CD11b Ab resulted in reduction of both CD11b$^+$ cells in tumors and expression of myeloid suppressive cell-associated genes as well as delayed tumor growth and prolonged survival. These effects could be further improved by 5-FU. Importantly, the combinatorial immunotherapy with ch14.18/CHO and 5-FU showed the strongest antitumor effects and superior survival rates. In conclusion, reduction of immune suppressive myeloid cells augments anti-NB efficacy of a ch14.18/CHO-based immunotherapy representing a new effective treatment strategy against GD$_2$-positive cancers.

ARTICLE HISTORY
Received 16 June 2020
Revised 23 September 2020
Accepted 9 October 2020

Keywords
neuroblastoma; immunotherapy; ch14.18/CHO; CD11b; suppressive myeloid cells; 5-FU

Introduction

Neuroblastoma (NB) is still a challenging cancer in childhood with poor survival and high relapse rates in the high-risk group,[1] despite the introduction of GD$_2$-directed immunotherapies with monoclonal Ab such as the chimeric ch14.18 produced in CHO cells.[2] Therefore, new treatment strategies are urgently needed.

Besides complement-dependent cytotoxicity (CDC), Ab-dependent cytotoxicity (ADCC) has been shown to be one of the major mechanisms of Ab-dependent antitumor effects,[3] mainly mediated by NK cells[4] and granulocytes.[5,6] To increase ADCC, IL-2, and GM-CSF were included in treatment protocols.[2,7] However, treatment of high-risk NB patients with the anti-GD$_2$ Ab ch14.18/CHO alone led to similar event-free survival (EFS) and overall survival (OS) compared to those patients who received a combined immunotherapy of ch14.18/CHO and IL-2.[2] Moreover, the efficacy of the cytokine-free treatment was nearly identical compared to the trial in which patients received dinutuximab (ch14.18 produced in SP2/0 cells), IL-2 and GM-CSF[7] emphasizing the need for more detailed investigation to clarify these unexpected results. Possible explanations could be a cytokine-mediated induction of immune suppressive cells such as regulatory T cells (T$_{reg}$) and cells of the myeloid lineage or immune checkpoint pathways, e.g., PD-1/PD-L1. We recently reported a strong induction of PD-L1 expression by both tumor- and immune cells following ADCC mediated by ch14.18/CHO and moreover, these effects were further increased by IL-2.[8] The induction of PD-L1 expression resulted in a strong decrease of the ADCC-mediated cytotoxicity. Investigation of the mechanisms associated with the ch14.18/CHO-dependent upregulation of the PD-1/PD-L1 checkpoint in NB revealed the involvement of CD11b$^+$ leukocytes. Experiments of CD11b blockade showed partial abrogation of PD-L1 expression resulting in restored ADCC,[8] suggesting an inhibitory/regulating role of these cells in NB.

Enrichment of suppressive cells of the myeloid lineage in NB has been shown previously in different animal models[9–12] and importantly, in patients.[13,14] Moreover, expression of the genes related to the suppressive cells has been reported to be associated with a poor clinical outcome.[13] This heterogeneous cell population is described as CD11b-positive (CD11b$^+$) immune suppressive myeloid cells in this report. These and our observations provide a rationale to explore therapeutic strategies depleting or reducing their suppressive mode of action.

In the present study, we investigated effects of ch14.18/CHO-mediated ADCC on production of tumor promoting cytokines and the expression of CD11b$^+$ myeloid cell-associated genes in tumor tissue. We further investigated the impact of an anti-CD11b Ab immunotherapy on gene expression, tumor growth and survival of treated mice. Based on the

CONTACT Nikolai Siebert nikolai.siebert@uni-greifswald.de Department of Pediatric Oncology and Hematology, University Medicine Greifswald, Greifswald 17475, Germany

facts that also NK cells express CD11b and treatment with anti-CD11b Ab can downregulate this antitumor effector cell population, we additionally treated mice with 5-FU that is a well-known anti-cancer agent (targets thymidylate synthase) depleting myeloid suppressive cells selectively when given at the concentration of 50 mg/kg.[15] Finally, we evaluated whether reduction of myeloid suppressive cells augments antitumor efficacy of a GD_2-directed immunotherapy with ch14.18/CHO.

Our data confirm accumulation of $CD11b^+$ myeloid cells in tumor tissue that was accompanied with a strong induction of immune suppressive genes. Application of anti-CD11b Ab reduced both, the number of $CD11b^+$ cells in tumors and expression levels of the genes analyzed, and it improved survival of treated mice indicating a negative impact of $CD11b^+$ myeloid cells in NB. Treatment with 5-FU further increased antitumor effects observed with anti-CD11b Ab, and this immune response was comparable to that of ch14.18/CHO. Interestingly, both ADCC mediated by ch14.18/CHO *in vitro* and ch14.18/CHO treatment of NB bearing mice *in vivo* resulted in a strong induction of the genes that are associated with myeloid suppressive cells. Importantly, by combining of the GD_2-directed treatment with 5-FU, both abrogation of gene expression in tumor tissue and the strongest antitumor effects compared to the respective single-agent treatments were observed. These data suggest that reduction of myeloid suppressive cells in combination with a GD_2-directed immunotherapy represents a more effective treatment strategy against GD_2-positive cancers.

Results

Tumor tissue is highly infiltrated by $CD11b^+$ cells

To investigate infiltration of advanced tumors (>600 mm^3) by $CD11^+$ cells, immunohistochemical (Figure 1(a-d)) and flow cytometry analyses of primary tumor tissue (Figure 1(e-f)) were performed.

Immunohistochemical analysis revealed that tumor tissues were infiltrated by leukocytes (staining against CD45) (Figure 1(a)) and by $CD11b^+$ cells (staining against CD11b) (Figure 1(c)). Detailed flow cytometry analysis confirmed our results of the immunohistochemical analysis showing that about 5% of all cells found in tumor tissue were leukocytes ($CD45^+/GD_2^-$) (Figure 1(f)) and that 53% of them were $CD11b^+$ (Figure 1f). Further analysis of the expression level of CD11b on these immune cells revealed heterogeneous expression patterns (Figure 1(e), right histogram) except for one population of about 50% cells showing high levels of CD11b (Figure 1(f)).

These results clearly show a strong accumulation of $CD11b^+$ immune cells in tumor tissue suggesting their key role in tumor development.

Release of cytokines induced by ch14.18/CHO-mediated ADCC

Based on the fact that ADCC strongly induces the expression of the immune checkpoint PD-L1,[8] we investigated whether ADCC mediated by ch14.18/CHO affects a production of the

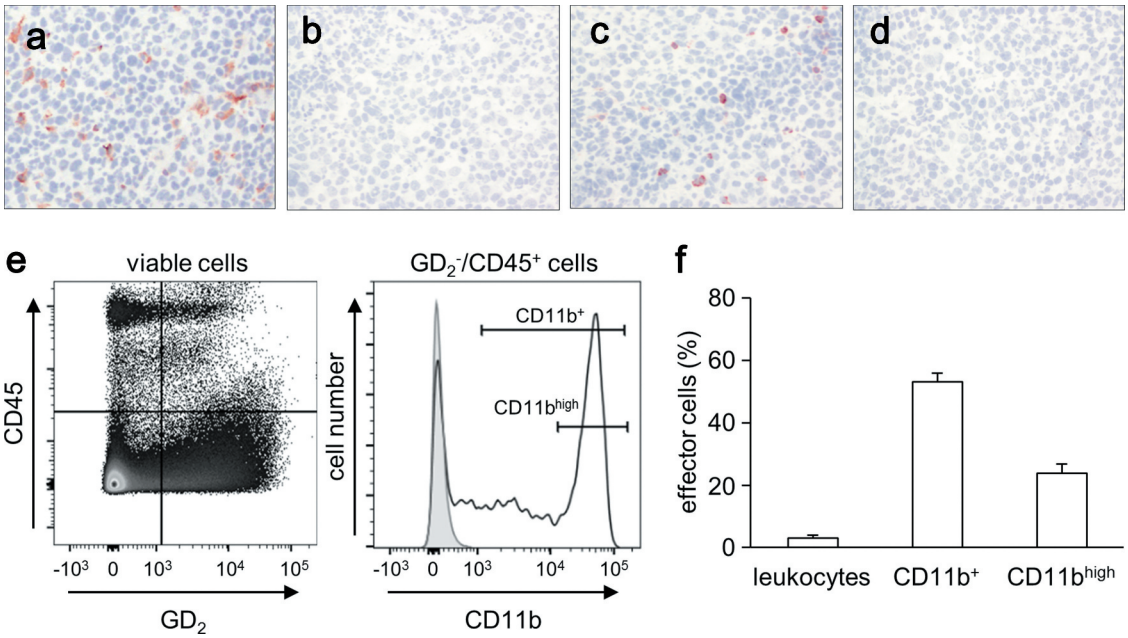

Figure 1. Evaluation of tumor infiltrating $CD11b^+$ cells. (a-d) Representative immunohistochemical images of tumor infiltrating leukocytes (a) and $CD11b^+$ cells (c) and respective negative controls (b and (d). Primary tumors obtained from A/J mice inoculated subcutaneously with NXS2-HGW NB cells were stained with either anti-CD45-(A) or anti-CD11b Ab (C) for detection of leukocytes and $CD11^+$ cells, respectively. Magnification of 100 ×. (e) Gating strategy of flow cytometric analysis of $CD11b^+$ cell subsets ($GD_2^-/CD45^+/CD11b^+$). A dot plot of GD_2 and CD45 expression showing a living cell fraction (left) was used to define a $GD_2^-/CD45^+$ cell population that was next characterized in terms of CD11b expression (open black curve) using a histogram (right). Isotype Ab served as a negative control (filled gray curve). (f) Quantitative analysis of leukocytes and $CD11b^+$ cells infiltrating primary tumors in untreated mice (0.9% NaCl; white columns). Leukocytes were calculated as a percent of the viable GD_2-negative CD45-positive cells relative to all viable cells detected in primary tumor tissue. Two subsets of $CD11b^+$ ($CD11b^+$ cells ($CD11b^+$) and cells showing high expression of CD11b ($CD11b^{high}$)) were calculated as a percent of viable $GD_2^-/CD45^+/CD11b^+$ cells relative to all viable leukocytes detected in tumor tissue.

cytokines known to modulate myeloid suppressive cells (M-CSF, GM-CSF, CCL2, CCL20, TGF-β, VEGF-A, IFN-γ, IL-1β, IL-4, IL-6, IL-8, and IL-10), we analyzed supernatants after 24 h cultivation of LAN-1 cells with leukocytes of healthy donors and subtherapeutic concentrations of ch14.18/CHO using a bead-based immunoassay.

Importantly, ADCC induced production of every cytokine analyzed (Figure 2) except for VEGF-A (tumor cell-derived, Figure 2, middle panel) and IL-10 (leukocyte-derived, Figure 2, lower panel), which both showed high baseline levels already prior to induction of ADCC. The strongest induction was observed for CCL2 (10.300.37 ± 1,735.88 vs. 1.13 ± 0.67 for LAN-1 and 1,287.92 ± 909.52 pg/ml for leukocytes), CCL20 (110.60 ± 20.18 vs. 0.66 ± 0.31 for LAN-1 and 7.69 ± 2.51 pg/ml for leukocytes) (Figure 2, upper panel), TGF-β (11.37 ± 3.70 vs. 1.95 ± 0.56 for LAN-1 and 3.01 ± 1.45 pg/ml for leukocytes) (Figure 2, middle panel), IL-4 (2.37 ± 0.43 vs. 0.09 ± 0.09 for LAN-1 and 0.55 ± 0.32 for leukocytes), IL-6 (216.31 ± 48.99 vs. 0.38 ± 0.24 for LAN-1 and 15.34 ± 5.46 for leukocytes) and IL-8 (8,464.24 ± 2,715.22 vs. 2.80 ± 0.34 for LAN-1 and 1,773.38 ± 1,188.27 for leukocytes) (Figure 2, lower panel). Although ADCC induced production of M-CSF, GM-CSF (Figure 2, upper panel), IFN-γ and IL-1β (Figure 2, lower panel), statistically significant differences compared with LAN-1 and leukocytes were found when ADCC was induced in the presence of IL-2 (Figure 2).

These data clearly show that GD_2-directed treatment leads to the production of the cytokines promoting immune suppressive cells of the myeloid lineage. Moreover, additional application of IL-2 further increased the observed effects.

Reduction of myeloid suppressive cells is effective against NB

To evaluate the role of myeloid suppressor cells in tumor development, we reduced their numbers with anti-CD11b and 5-FU in the syngeneic murine tumor model (Figure 3 (a)). As myeloid suppressive cells express CD11b, we first treated mice with anti-CD11b Ab. We also used 5-FU at the concentration of 50 mg/kg that has been reported to deplete myeloid suppressor cells selectively.[15]

Untreated control mice showed an exponential tumor growth starting on day 11 after tumor cell injection with an average volume of 600 mm^3 on day 21 (Figure 3(b)). Treatment of mice with anti-CD11b Ab resulted in a statistically highly significant reduction of $CD11b^+$ cells in tumor tissue (Figure 3 (c)). This translated into a statistically significant delay in tumor growth starting on day 17 (Figure 3(b)) with a twofold decrease on day 21 compared to controls. Of note, we observed toxicity after application of anti-CD11b Ab limiting usage of this agent in combination with other immunotherapeutics. Similar to the anti-CD11b treatment, application of 5-FU Ab

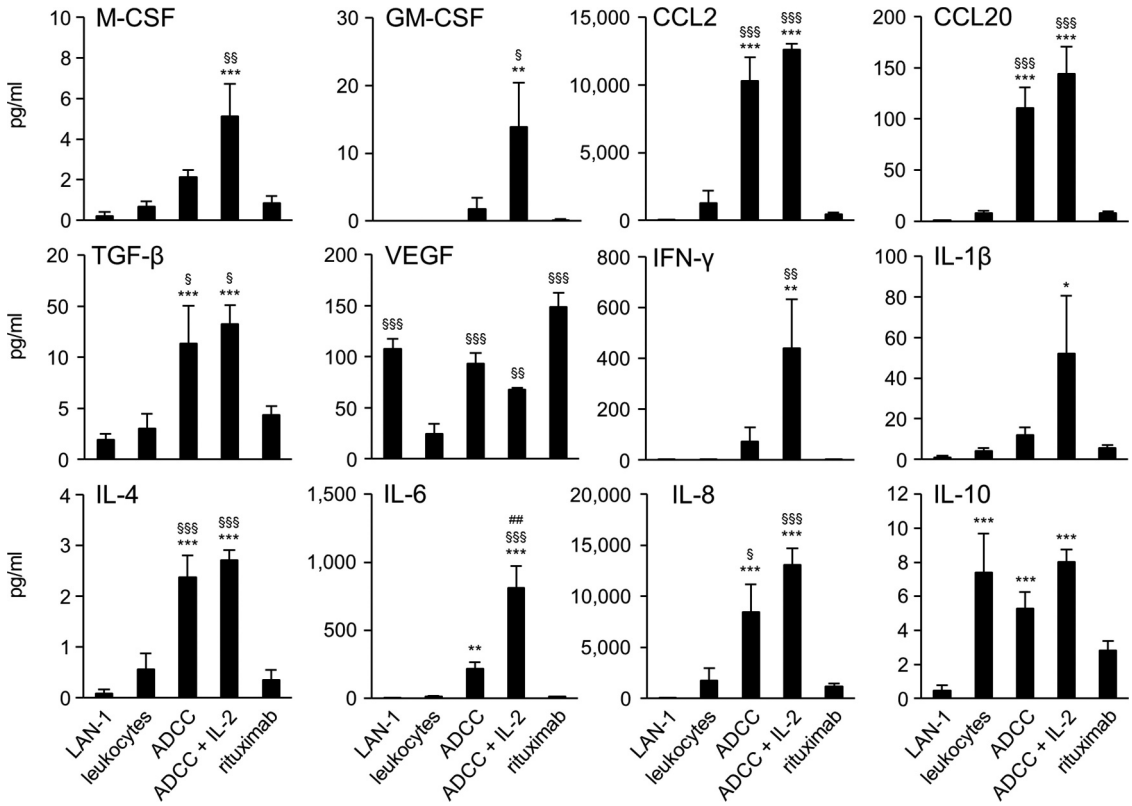

Figure 2. Effects of ADCC culture conditions on cytokine production by human NB cells and leukocytes. Concentrations of the cytokines M-CSF, GM-CSF, CCL2 and CCL20 (upper panel), TGF-β, VEGF, IFN-γ and IL-1β (middle panel) and IL-4, IL-6, IL-8 and IL-10 (lower panel) were determined by flow cytometry in supernatants 24 h after induction of GD_2-directed ADCC in the presence or absence of IL-2. Rituximab served as control. Data represent mean values ± SEM of at least two independent experiments. Statistical analysis was performed with ANOVA followed by appropriate post hoc comparison test. To show IL-2-dependent impact on cytokine production, *t*-test was used. $^{*}P < .05$ vs. LAN-1, $^{**}P < .01$ vs. LAN-1, $^{***}P < .001$ vs. LAN-1, $^{\S}P < .05$ vs. leukocytes, $^{\S\S}P < .01$ vs. leukocytes, $^{\S\S\S}P < .05$ vs. leukocytes, $^{\#\#}P < .01$ vs. ADCC.

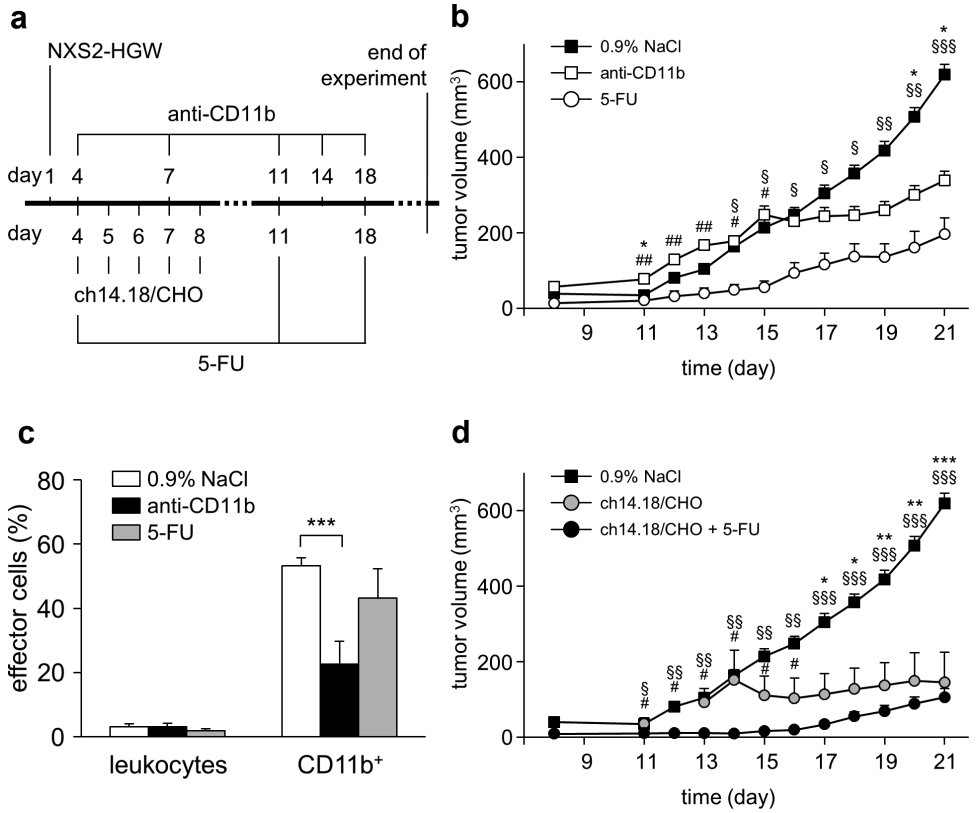

Figure 3. Antitumor effects of the ch14.18/CHO treatment in combination with reduction of suppressive myeloid cells *in vivo*. (a) Schematic overview of the treatment protocol. Four days after tumor cell injection, mice received either ch14.18/CHO or anti-CD11b Ab or 5-FU or combination of ch14.18/CHO and 5-FU. (b) Analysis of tumor growth in mice treated with either anti-CD11b Ab (open squares) or 5-FU (open circles). Controls received 0.9% NaCl (closed squares). Data are shown as mean values ± SEM. Statistical analysis of differences between anti-CD11b and control, 5-FU and control as well anti-CD11b and 5-FU groups was performed with one-tailed t-test: $^{*}P < .05$ for 0.9% NaCl vs. anti-CD11b; $^{\S}P < .05$, $^{\S\S}P < .01$, $^{\S\S\S}P < .001$ for 0.9% NaCl vs. 5-FU; $^{\#}P < .05$, $^{\#\#}P < .01$ for anti-CD11b vs. 5-FU. (c) Analysis of tumor infiltrating effector cells of mice treated with anti-CD11b Ab (anti-CD11b, black columns) or 5-FU (5-FU, gray columns) in comparison with the untreated controls (0.9% NaCl, white columns). Leukocytes shown in % of all viable $CD45^{+}/GD2^{-}$ cells and $CD11b^{+}$ cells shown in % of all viable $CD45^{+}/CD11b^{+}/GD2^{-}$ cells were assessed in tumor tissue using flow cytometry analysis. To show impact of anti-CD11b and 5-FU treatments on effector cell count, t-test was used. $^{***}P < .001$ vs. 0.9% NaCl. (d) Analysis of tumor growth in mice treated with either ch14.18/CHO alone (gray circles) or ch14.18/CHO in combination with 5-FU (closed circles). Controls received 0.9% NaCl (closed squares). Data are shown as mean values ± SEM. Statistical analysis of differences between ch14.18/CHO and control, combined treatment (ch14.18/CHO + 5-FU) and control as well as combined treatment (ch14.18/CHO + 5-FU) and 5-FU groups was performed with one-tailed *t*-test: $^{*}P < .05$, $^{*}P < .01$, $^{*}P < .001$ for 0.9% NaCl vs. ch14.18/CHO group; $^{\#}P < .05$ for ch14.18/CHO vs. combined treatment group (ch14.18/CHO + 5-FU); $^{\S}P < .05$, $^{\S\S}P < .01$, $^{\S\S\S}P < .001$ for 0.9% NaCl vs. combined treatment group (ch14.18/CHO + 5-FU).

led also to a reduction of tumor infiltrating CD11b+ cells (Figure 3(c)). However, the differences between the groups were statistically not significant. Interestingly, there was even a stronger antitumor effect when mice were treated with 5-FU (Figure 3(b)). A statistically significant delay of tumor growth was observed already on day 14 and tumors were even threefold smaller on day 21 compared to untreated mice.

Comparing tumor volumes of the anti-CD11b with the 5-FU group at the respective days revealed a significant differences starting on day 11 with superior antitumor effects for 5-FU (Figure 3(b)). The tumor volumes in 5-FU treated mice were fourfold and twofold smaller than in anti-CD11b mice on days 11–15 and 16–21, respectively.

Together, these results show antitumor efficacy of both agents anti-CD11b Ab and 5-FU on tumor growth with superior effects of 5-FU.

5-FU antitumor effects are partially attributed to its toxic effects on tumor cells

Next, to investigate whether the observed antitumor effects of 5-FU were due to its direct cytotoxic effects on the NB cells NXS2-HGW served for tumor establishment *in vivo*, an XTT-based assay was performed. Additionally, we analyzed 5-FU effects on effector cells. Incubation of NXS2-HGW cells *in vitro* with different concentrations of 5-FU (final concentrations of 5.6, 16.7, 50, 150, 450, and 1350 µg/ml) showed some reduction of cell viability compared to the untreated control (Figure 4). However, the differences between the groups were statistically not significant. These results suggest that the antitumor effects of 5-FU can be explained mainly by its ability to reduce suppressive myeloid cells, as has been previously shown, but also probably by some direct toxic effects on tumor cells observed in the present study.

Additionally, we investigated whether 5-FU has any direct impact on effector cells *in vitro*. For that, we incubated murine leukocytes with different concentrations of 5-FU as described for tumor cells and observed similar cell viability with untreated controls (Figure 4). Although, incubation of leukocytes with higher 5-FU concentrations (150, 450, and 1,500 µg/ml) resulted in a slightly decreased viability indicating some toxic effects of 5-FU on effector at these concentrations, the differences between the 5-FU groups and untreated controls were not statistically different. Moreover, we analyzed whether

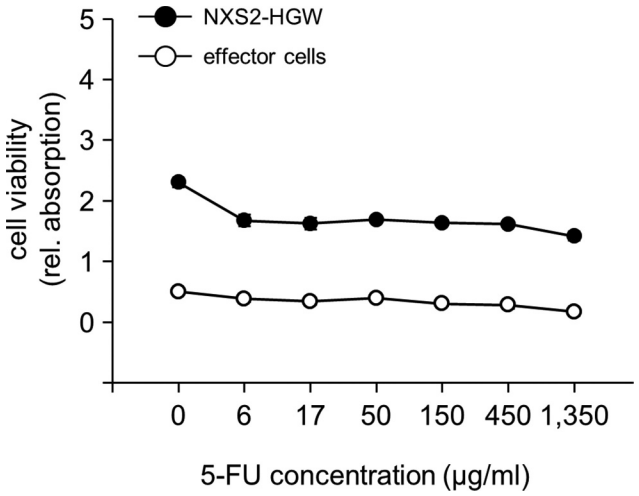

Figure 4. Analysis of 5-FU impact on viability of tumor and effector cells *in vitro*. To analyze direct 5-FU impact on the viability of NB and effector cells, NXS2-HGW cells served for tumor establishment (closed circles) and leukocytes isolated from spleens of healthy mice (open circles) were incubated with six different 5-FU concentrations in the range of 6–1500 µg/ml followed by analysis of cell viability with XTT-based viability assay. Data represent mean values ± SEM of at least three independent experiments. When error bars are not visible they are covered by the symbol. Differences between the groups were statistically not significant. Kruskal-Wallis one way analysis of variance on Ranks.

5-FU affects $CD4^+$ and $CD8^+$ cells (data not shown) and did not find any change of cell viability compared with untreated controls. These results suggest that 5-FU, if any, only marginally affects the viability of the effector cells directly.

Reduction of suppressive myeloid cells augments antitumor effects of ch14.18/CHO on tumor growth

Finally, based on the promising results of the two treatment strategies, namely the immunotherapy with the chimeric anti-GD_2 Ab ch14.18/CHO[2,8] and a reduction of myeloid suppressive cells shown in the present study (Figure 3), we combined both immunotherapies to augment the antitumor efficacy observed by the respective single-agent treatment. The rationale to additionally reduce myeloid suppressive cells was further based on our results of the *in vitro* analysis of an ADCC-dependent cytokine production mediated by ch14.18/CHO showing a strong induction of those cytokines that are involved in a modulating of myeloid suppressive cells (Figure 2). Since 5-FU treatment was more effective than anti-CD11b Ab, NK cells mediating antitumor effects of anti-GD_2 Ab express CD11b and anti-CD11b treatment showed toxicity in mice, we used 5-FU in the combinatorial treatment.

As expected, a single-agent treatment with ch14.18/CHO resulted in a strong tumor growth delay compared with both untreated mice and mice treated with anti-CD11b Ab showing similar antitumor effects as in the 5-FU group (Figure 3(b,d)). The highest reduction of tumor volumes was observed between day 11 and 15 (Figure 3(b)) for 5-FU and between day 17 and 21 for ch14.18/CHO (Figure 3(d)). This could be explained by different action mechanisms of these drugs and should be taken into account by planning of combinatorial immunotherapies including both agents.

Most important, the strongest tumor inhibiting effect was observed in mice treated with a combination of ch14.18/CHO and 5-FU showing a steady delay in tumor growth during the whole treatment period (Figure 3(d)). The differences between tumor volumes in the mice treated with either ch14.18/CHO alone or ch14.18/CHO + 5-FU were statistically significant for the time period between days 11 and 16.

Altogether, these results clearly show that the observed antitumor efficacy of the GD_2-directed immunotherapy with ch14.18/CHO can be further increased by a reduction of suppressive myeloid cells.

Reduction of suppressive myeloid cells further improves overall survival of mice treated with ch14.18/CHO

Next, we evaluated efficacy of both ch14.18/CHO and 5-FU single-agent treatments as well as the combinatorial immunotherapy on survival of the treated mice. We observed a significantly improved survival of the mice treated with either the 5-FU- or ch14.18/CHO single-agent treatment (Figure 5(a)). The overall survival (OS) probabilities on day 28 of the 5-FU- and ch14.18/CHO mice were 40% and 70% compared with controls (20%), respectively.

Notably, we observed a superior survival probability in those mice that received both agents (Figure 5(a)). All mice of the combinatorial treatment group survived until day 28. However, a statistical analysis revealed significant differences only between the survival probabilities of the combinatorial group and the 5-FU as well as control group.

These results could be confirmed by the analysis of a tumor regression status on day 28. Forty percent of the mice treated with the combination of ch14.18/CHO and 5-FU achieved a complete response compared to the ch14.18/CHO group, where 10% of the mice responded (data not shown). In contrast, all mice of the 5-FU group showed evidence of disease suggesting a superior anti-NB efficacy of ch14.18/CHO compared to 5-FU.

In summary, we could clearly show beneficial efficacy of the combinatorial immunotherapy with ch14.18/CHO and reduction of myeloid suppressive cells against NB *in vivo*.

Tumor development results in a strong induction of myeloid suppressive cell-associated and modulating genes that can be reversed by anti-CD11b- and 5-FU treatments

We further investigated the expression of the myeloid suppressive cell-associated and modulating genes encoding M-CSF, M-CSFr, GM-CSF, CCL2, TGF-β, IL-1β, IL-4, IL-6, IL-6 r, IL-8, IL-10, VEGF-A, Arg1, IDO, NOS2, and IFN-γ by RT-PCR (Figure 5(b)).

Interestingly, analysis of the gene expression in the NB cells NXS2-HGW that were used for tumor establishment revealed a strong baseline mRNA expression of tumor promoting M-CSF, IL-6, TGF-β, and VEGF-A suggesting tumor cell-dependent induction of myeloid cells (M-CSF), inhibitory effects on antitumor response (TGF-β) and promoting tumor angiogenesis (VEGF-A).

Importantly, primary tumors induced by NXS2-HGW cells showed a strong induction of all genes analyzed *in vivo* (Figure

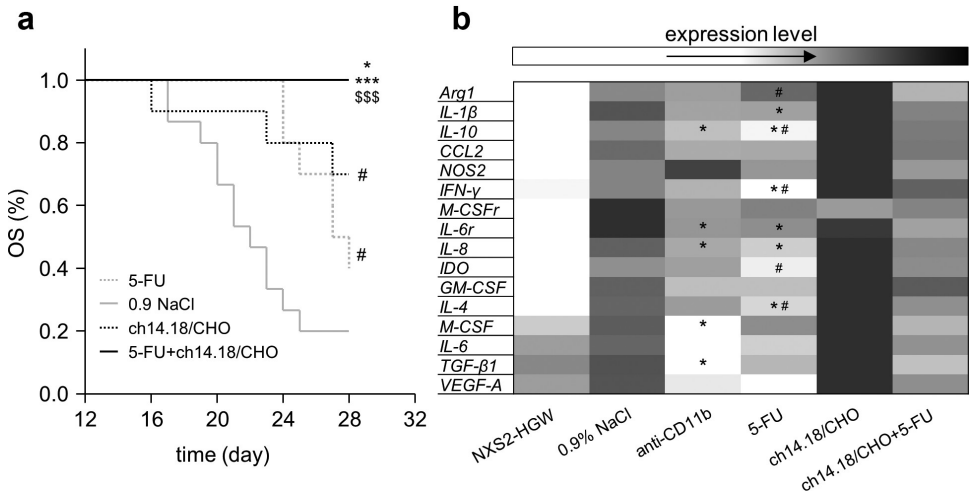

Figure 5. Impact of the ch14.18/CHO treatment and reduction of suppressive myeloid cells on survival and gene expression. The GD_2 expressing murine NB cells NXS2-HGW were injected subcutaneously into A/J mice followed by the treatment with the chimeric anti-GD_2 Ab ch14.18/CHO, anti-CD11b Ab, 5-FU, or combination of ch14.18/CHO and 5-FU. (a) Comparison of OS probabilities of mice treated with either ch14.18/CHO alone (black dashed line) or 5-FU alone (gray dashed line) or ch14.18/CHO in combination with 5-FU (black solid line) with control mice (0.9% NaCl, gray solid line). Death ahead of schedule and a tumor volume of 750 mm^3 were defined as event. LogRank test. $^{*}P < .05$ vs. ch14.18/CHO, $^{***}P < .001$ vs. 5-FU, $^{\$\$\$}P < .001$ vs. 0.9% NaCl, $^{\#}P < .05$ vs. 0.9% NaCl. (b) Comparison of mRNA expression levels of suppressive myeloid cell-associated and modulating genes between primary tumor tissue and NB cells NXS2-HGW used for tumor establishment. Tumor samples were collected from tumor bearing mice treated with ch14.18/CHO, anti-CD11b, 5-FU, or ch14.18/CHO in combination with 5-FU as well as control mice. Expression levels of Arg1, IL-1β, IL-10, CCL2, NOS2, IFN-γ, M-CSFr, IL-6 r, IL-8, IDO, GM-CSF, IL-4, M-CSF, IL-6, TGF-β1, and VEGF-A were determined using RT-PCR analysis relative to the internal control GAPDH and are represented as colors. The color spectrum between light- and dark gray was used to represent the different levels of expression with light gray for low- and dark gray for high expression of the respective gene. Statistical analysis of expression level differences between anti-CD11b and control, 5-FU and control, anti-CD11b and 5-FU as well as ch14.18/CHO and ch14.18/CHO in combination with 5-FU groups was performed with one-tailed *t*-test: $^{*}P < .05$ vs. 0.9% NaCl, $^{\#}P < .05$ vs. anti-CD11b.

5(b), 0,9% NaCl), even a further increase of those genes that showed a strong baseline expression by tumor cells only, underlining tumor microenvironment-dependent induction of the genes that are known to be associated with myeloid suppressive cells.

Next, we addressed whether reduction of myeloid suppressive cells by anti-CD11b Ab or 5-FU abrogates tumor-dependent induction of these genes.

Targeting myeloid cells with anti-CD11b Ab resulted in a strong decrease of mRNA levels of all analyzed genes (Figure 5(b)) in tumors compared to untreated controls. The differences between the groups were found to be significant for IL-6 r, IL-10, IL-8, M-CSF, and TGF-β. Similar results could be observed for the 5-FU group compared to the untreated controls showing a strong decrease of mRNA expression of all genes analyzed as well (Figure 5(b)). Moreover, the expression levels of IL-10, IDO, and IL-4 were found to be further decreased in the 5-FU group compared to the anti-CD11b mice. Interestingly, we found a statistically significant increase of Arg1 and decrease of IFN-γ gene expression in tumors of 5-FU mice compared to the anti-CD11b group.

To investigate whether observed ADCC-dependent induction of tumor promoting cytokines mediated by ch14.18/CHO *in vitro* (Figure 2) translates into *in vivo* effects, we determined mRNA expression of the above mentioned genes in tumor tissue of the mice treated with ch14.18/CHO (Figure 5(b)).

Our *in vitro* analysis of ADCC-dependent cytokine secretion could be clearly confirmed by the RT-PCR analysis of gene expression in tumor tissue. Compared with untreated controls we detected after the treatment with ch14.18/CHO even a stronger induction of all genes analyzed except for M-CSFr (Figure 5(b)). These data indicate an accumulation of immune cells with tumor promoting mode of action in tumor tissue after treatment with ch14.18/CHO and underline the need for reduction of these cells when combined with a GD_2-directed treatment.

Finally, we investigated effects of the combinatorial immunotherapy with ch14.18/CHO and reduction of myeloid suppressive cells on mRNA expression of these genes. As hypothesized, a combinatorial treatment with ch14.18/CHO and 5-FU resulted in a downregulation of ch14.18/CHO-dependent induction of all the genes analyzed (Figure 5(b)). Altogether, reduction of myeloid suppressive cells abrogates ch14.18/CHO-dependent induction of the genes that are known to modulate or to be associated with myeloid suppressive cells in tumor tissue emphasizing the need for a co-treatment with agents reducing inhibitory effects of immune system.

Expression levels of myeloid suppressive cell-associated and modulating genes correlate with tumor growth

To address whether a stage of tumor development has any impact on mRNA expression of myeloid suppressive cell-associated and modulating genes, we compared mRNA expression levels from tumors with high- (>600 mm^3) and low volumes (<500 mm^3) representing late and early stages of a tumor development, respectively using RT-PCR analysis (Figure 6). As expected, compared with low volume tumors, in tumors of the late development stage we observed higher expression levels of all genes analyzed except for CCL2 and IDO showing similar expression levels in both groups. The

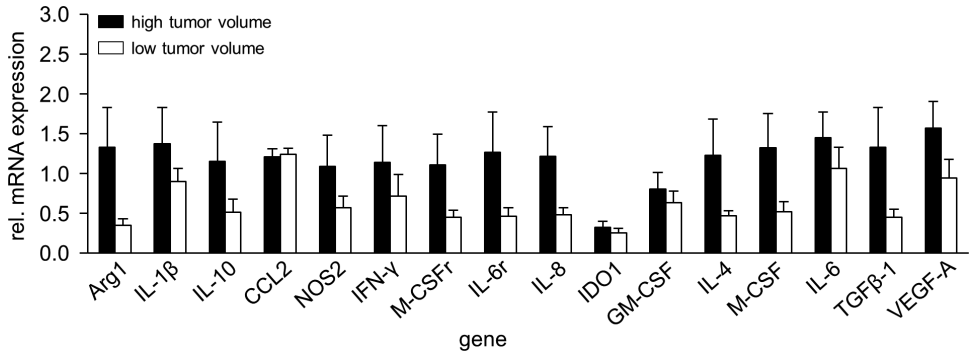

Figure 6. Comparison of gene expression in high- and low volume tumors. To show impact of a tumor volume on mRNA gene expression, samples from tumors showing high- (>600 mm^3, black columns) and low volumes (<500 mm^3, white columns) were analyzed with RT-PCR analysis. Expression levels of mRNA were determined relative to the internal control GAPDH. Data are shown as mean of relative mRNA expression from at least three independent experiments.

strongest differences were found for Arg1, IL-4, IL-6 r, IL-8, M-CSF, and TGF-β showing about 3-fold increased mRNA expression in tumors of the later development stage compared to the early stage. For IL-1β, IL-10, NOS2, IFN-γ, M-CSFr, and VEGF-A, we observed about twofold differences between the groups. However, these differences were statistically not significant.

These data suggest a correlation between the stage of a tumor development and expression levels of the genes involved in tumor promoting mechanisms.

Discussion

Immunotherapeutic strategies based on the application of anti-GD_2 Ab have shown promising results in treatment of high-risk NB.[16] However, response rates from these immunotherapies vary, and some patients still have a poor outcome. Possible explanations may be immune-suppressive effects mediated by the tumor as well as regulatory mechanisms following immunotherapeutic intervention, such as upregulation of immune checkpoints. We have previously shown induction of the immune checkpoint PD-L1 on both tumor and effector cells by ADCC mediated by the chimeric anti-GD_2 Ab ch14.18/CHO.[8] Most notably, tumor cells harvested after 24 h ADCC were resistant against antitumor effects of the therapeutic Ab and could be only killed when ch14.18/CHO treatment was combined with the blockade of the PD-1/PD-L1 pathway.[8] In this context, we observed that additional treatment with anti-CD11b Ab resulted in a decrease of PD-L1 expression on tumor cells induced by ADCC and improved antitumor effects of ch14.18/CHO, suggesting involvement of $CD11b^+$ immune cells in immune suppressive effects.

In the present study, we could confirm our previous *in vitro* results by showing a strong infiltration of tumor tissue by $CD11b^+$ immune cells *in vivo* (Figure 1). Furthermore, we observed that ch14.18/CHO-mediated ADCC induced expression of M-CSF, GM-CSF, CCL2, CCL20, TGF-β, IL-1β, IL-4, IL-6, and IL-8 and interestingly, of IFN-γ (Figure 2). These cytokines have been shown to drive development of myeloid suppressive cells and are associated with a tumor promotion.[17] These results suggest that besides tumor cell elimination, immunotherapies also lead to activation of various regulation mechanisms dampening antitumor efficacy of therapeutic agents.

Over the last few years, there has been an increasing interest in characterization and understanding of the role of $CD11b^+$ immune cells that exert immune suppressive functions. Most of these cells are comprised of a heterogeneous immature myeloid cell population inhibiting T- and NK-cell activity and promoting tumor growth, development of metastases, and contributing to resistance to immunotherapy.[17]

Based on our results of CD11b-dependent induction of PD-L1 on tumor and effector cells under GD_2-directed treatment and a strong infiltration of tumor tissue by $CD11b^+$ immune cells, we addressed whether their reduction augments antitumor effects of ch14.18/CHO. As hypothesized, a combination of both treatment strategies showed superior antitumor effects compared to the respective single-agent treatment. To clarify the question which $CD11b^+$ cell population or cell populations is or are responsible for the immune suppressive effects observed in the present work, more detailed investigations are needed. Here, functional assays showing direct suppressive effects of different populations of $CD11b^+$ cells on antitumor effector cells such as NK- and $CD8^+$ cells are promising options. Although treatment of mice with anti-CD11b Ab showed here clear therapeutic effects, application of 5-FU was more effective against NB. We used 5-FU at the concentration of 50 mg/kg that has been shown to selectively deplete only myeloid suppressive cells.[15] Moreover, at this concentration, 5-FU does not affect NK cells[15] that are known to be a major cell population mediating antitumor mechanisms of therapeutic Ab. We previously showed that the blockade of NK cells resulted in a complete abrogation of the observed antitumor effects by ch14.18/CHO,[3] confirming the major role of NK cells in mediation of antitumor effects of an anti-GD_2 treatment. Moreover, we also observed in the present study that 5-FU has some direct toxic effects on tumor cells suggesting both action mechanisms mediating 5-FU antitumor efficacy.

Although treatment of mice with ch14.18/CHO showed antitumor efficacy, we observed in tumor tissue a strong induction of the myeloid suppressive cell-associated genes encoding M-CSF, M-CSFr, GM-CSF, CCL2, TGF-β, IL-1β, IL-4, IL-6, IL-6 r, IL-8, IL-10, VEGF-A, Arg1, IDO, NOS2, and, surprisingly, IFN-γ (Figure 5), which is in line with our *in vitro*

findings (Figure 2). These genes have been reported to drive immune suppression in various cancers via direct inhibition of antitumor effector cells and/or promoting immune suppressive cells such as T_{reg} and suppressive cells of the myeloid lineage and/or inducing immune checkpoints.[17] Thus, induction of antitumor response is accompanied with activation of strong regulatory mechanisms supporting tumor promoting effects of tumor microenvironment.

Although targeting of GD_2 with monoclonal Ab is effective against NB,[16] our results suggest to combine Ab immunotherapies with strategies reducing myeloid suppressive cells. Indeed, we here and others showed that NB growth could be delayed by the agents reducing myeloid suppressive cells such as 5-FU,[11] Vorinostat,[12] Polyphenon E[14], or low-dose aspirin.[10]

Unexpectedly, we found in the present study strong induction of INF-γ in tumor tissue of untreated mice, higher INF-γ levels in tumors with larger volumes (Figure 6) and that reduction of myeloid suppressive cells resulted in a decrease of INF-γ (Figure 5). Altogether, these results suggest a possible involvement of this cytokine in tumor promoting mechanisms. These unexpected results are in line with the studies showing INF-γ-dependent promotion of ovarian cancer[18] and melanoma[19] via induction of the immune checkpoint pathway PD-1/PD-L1 not only by tumor cells but also by immune cells. Moreover, CTLA-4 expression by melanoma cells by INF-γ has been reported to mediate immune evasion.[20] Most notably, INF-γ has been shown to be involved in accumulation of myeloid suppressive cells within tumors[21] further confirming tumor promoting effects of this cytokine. However, based on vast studies praising INF-γ as the cytokine of antitumor immunity, further investigations are needed to clarify these unexpected results.

In summary, we show here that treatment of NB with ch14.18/CHO leads to a strong induction of myeloid suppressive cells and that reduction of these cells augments antitumor efficacy of the ch14.18/CHO-based immunotherapy. Our findings provide a rationale for a promising combinatorial strategy to effectively reduce NB growth and further improve survival on NB patients.

Methods

Ethic statement

All procedures involving human participants were performed in accordance with the ethical standards of the institutional and national research committee and with the 1964 Helsinki declaration and its later amendments or comparable ethical standards. Informed consent was obtained from all individual participants (Ethics Board of the Medical Faculty of the University Greifswald, approval code number: BB 014/14, 24.01.2014). All procedures involving animal experiments were approved by the animal welfare committee (Landesamt für Landwirtschaft, Lebensmittelsicherheit und Fischerei Mecklenburg-Vorpommern, LALLF M-V, approval code number: 7221.3-1-049/15, 27.11.2015) and supervised by the commissioner for animal welfare at the University Medicine Greifswald representing the Institutional Animal Care and Use Committee (IACUC).

Cell lines and effector cells

To investigate ADCC-mediated induction of cytokine production *in vitro*, the human GD_2-positive NB cell line LAN-1 and leukocytes of a healthy donor were cultivated as previously reported.[8] Briefly, LAN-1 were incubated with effector cells and ch14.18/CHO for 24 h. Effector cells were first isolated from sodium-heparin blood samples of a healthy donor using erythrocyte lysis buffer (10 min, RT, 0.15 M ammonium chloride, 10 mM potassium bicarbonate, 0.1 mM ethylenediaminetetraacetic acid, pH 7.4) and washed twice (1× PBS, 5 min, 300 × g, RT), followed by cell counting and evaluation of cell viability. Then, 0.5×10^6 LAN-1 cells were harvested and incubated with effector cells at effector-to-target (E:T) ratio of 10:1 for 24 h in the presence of ch14.18/CHO at the final concentration of 10 ng/ml. Moreover, we evaluated impact of IL-2 using cell culture medium supplemented with 100 IU/ml of IL-2. Additionally, the effect of ch14.18/CHO on NB- and effector cells as well as effects of NB cells on effector cells and *vice versa* of effector cells on NB cells were investigated. Finally, to confirm ch14.18/CHO-mediated impact of ADCC, incubation with the anti-idiotype ganglidiomab[22] was additionally performed. To evaluate antitumor efficacy of the new immunotherapies *in vivo*, the murine NB cells NXS2-HGW that grow in immunocompetent A/J mice were used.[8] These cells were established using a paternal cell line NXS2[23] as described previously[8] and express the NB-specific markers GD_2, tyrosine hydroxylase and MYCN as well as PD-L1. For cultivation, DMEM supplemented with 4.5 g/l glucose, 2 mM stable glutamine, 10% FCS, 100 U/ml penicillin and 0.1 mg/ml streptomycin was used. Prior to cultivation, mycoplasma contamination analysis was performed for every cell line using MYCOALERT detection Kit (Lonza Cologne GmbH, LT07-318). Only mycoplasma negative cell lines were used for experiments. All cell lines were passaged not more than 30 times.

To investigate direct effects of 5-FU on effector cells, murine splenocytes were used. Briefly, mice spleens were mechanically dispersed using 70 µm cell strainer, washed twice with 1× PBS (300 × g, 5 min, RT) followed by cell counting and evaluation of cell viability. For cultivation, RPMI supplemented with 4.5 g/l glucose, 2 mM stable glutamine, 10% FCS, 100 U/ml penicillin and 0.1 mg/ml streptomycin, 50 µM 2-mercaptoethanol and 100 IU/ml rIL-2 was used.

Murine tumor model

To evaluate antitumor efficacy of the immunotherapy with ch14.18/CHO in combination with reduction of myeloid suppressive cells, a lethal syngeneic murine NB model[8,23] was used. The mice were granted a two week acclimatization time, accommodated in groups of maximum 6 animals in standard animal laboratories (12 h light/dark cycle, 20°C ± 2°C room temperature, 60% ± 20% humidity) with *ad libitum* access to

water and standard laboratory chow. Subcutaneous tumors were established on the left ventral flank of female A/J mice (10 weeks of age, ≥20 g, Charles River Laboratories, Sulzfeld, Germany) by injecting 2×10^6 tumor cells (≥95% viability).

For all *in vivo* experiments performed with 12 mice per experimental group, mice were randomized prior to tumor cell injection. Mice were untreated (0.9% NaCl, i.p.) or treated with ch14.18/CHO alone (provided by Polymun Scientific, Klosterneuburg, Austria), 15 mg/kg, i.p., days 4, 5, 6, 7, and 8 after tumor cell injection), anti-CD11b Ab alone (Bio X Cell, West Lebanon, NH, USA, clone M1/70, 25 mg/kg, i.p., days 4, 7, 11, 14, and 18), 5-FU alone (Merck, Darmstadt, Germany, 50 mg/kg, i.p., days 4, 11, and 18), or ch14.18/CHO and 5-FU. Based on our previous observations showing lack of antineuroblastoma efficacy of isotype control Ab,[3] we used in this work only one control group that received 0.9% NaCl instead of the respective isotype control Ab.

Tumor- and/or treatment burden parameters were assessed every two days after tumor cell injection and daily starting on day 11 as previously described.[8] Tumor volume was calculated according to the formula: (length □ width □ height)/2. Mice were sacrificed when tumors exceeded 750 mm^3. For those mice killed ahead of schedule, tumor volume data of the last measurement were included into the calculation of the group-specific average volumes at the subsequent time points. Overall survival probability was defined as described previously.[8]

Flow cytometry

To identify tumor infiltrating $CD11b^+$ leukocytes (GD_2^-/$CD45^+$/$CD11b^+$), flow cytometry analysis was used. For this, a single cell suspension was prepared from resected primary tumors using a cell strainer (70 µm). Staining was performed with Alexa647-labeled anti-GD_2 Ab,[8] FITC-labeled anti-mouse/human CD11b Ab (1.25 µg/ml, clone M1/70, BioLegend San Diego, CA, USA) and PE/Cy7-labeled anti-mouse CD45 Ab (0.67 µg/ml, clone 30-F11, BioLegend San Diego, CA, USA) and respective isotype controls.

To exclude dead cells, 4 µl of a 0.1 mg/ml 4′,6-diamino-2-phenylindole (DAPI) solution were added 5 min prior to acquisition using a BD CANTO II cytometer and FACS Diva software. Data were analyzed with FlowJo V10 software. $CD11b^+$ cell subset was calculated as a percent of GD_2^-/$CD45^+$ cells within the living cell fraction.

Immunohistochemistry

To show infiltration of tumor tissue by leukocytes ($CD45^+$) and $CD11b^+$ cells, immunohistochemical analysis was performed. For this, primary tumor samples were first frozen in liquid nitrogen using O.C.T. compound medium and cryo-sections (6 µm) were then analyzed. Fixation was accomplished using acetone (10 min; −20°C) followed by 20 min air drying and three wash steps with 1× TBS (3 min). For immunohistochemical staining, cryo-sections were incubated with 3% H_2O_2 for 20 min at RT, washed three times and treated with 3% BSA/TBS (20 min, RT) and 5% goat serum/TBS (20 min, RT) each followed by three wash steps. Next, purified anti-mouse/human CD11b (3.33 µg/ml, clone M1/70, BioLegend San Diego, CA, USA) or purified anti-mouse CD45 (10 µg/ml, clone 30-F11, BioLegend San Diego, CA, USA) in 3% BSA/TBS was used for 1 h staining at RT followed by another 3 wash steps. Then, peroxidase-conjugated secondary Ab goat anti-rat IgG (0.8 µg/ml, BioLegend San Diego, CA, USA) in 1% BSA/TBS was incubated for 20 min at RT and washed three times. After incubation with the 3-Amino-9-ethylcarbazol (AEC) substrate solution (0.05% AEC, 0.015% H_2O_2 in 0.05 M acetate buffer, pH 5.5) sections were washed, counterstained with Mayer's hemalum solution for 3 min at RT, mounted with Mowiol 4–88 and examined by light microscopy. Incubation with 3% BSA/TBS without Ab serves as negative control.

Evaluation of cytokine production under ADCC culture conditions

To evaluate impact of ch14.18/CHO-mediated ADCC culture conditions on production of the cytokines M-CSF, GM-CSF, CCL2, CCL20, TGF-β, VEGF-A, IFN-γ, IL-1β, IL-4, IL-6, IL-8, and IL-10 by human NB cells and leukocytes, a cytokine-specific bead-based immunoassay (BioLegend San Diego, CA, USA) was conducted using 25 µl supernatant according to the manufacturers' protocol (Custom Legendplex™ panel, BioLegend San Diego, CA, USA). ADCC was induced by sub-therapeutic concentrations of ch14.18/CHO as previously reported[8] and briefly described above.

RT-PCR

To investigate expression of $CD11b^+$ myeloid cell-associated and modulating genes (M-CSF, M-CSFr, GM-CSF, CCL2, TGF-β, IL-1β, IL-4, IL-6, IL-6 r, IL-8, IL-10, VEGF-A, Arg1, IDO, NOS2, and IFN-γ) in tumor tissue, gene-specific primers (Table 1) were designed by the online primer design tool Primer3, Primer-BLAST provided by the NCBI or recent reports.[24–27] The housekeeping gene glyceraldehyde 3-phosphate dehydrogenase (GAPDH) was used as an internal control. Primer-specific PCR programs are listed in the Table 1.

First, total RNA was isolated using the RNeasy Mini Kit (QIAGEN GmbH, Hilden, Germany) followed by RT-PCR analysis. To assess gene-specific expression levels, agarose gel electrophoresis (ImageLab™ Software, BioRad Laboratories GmbH, Munich, Germany) and densitometric analysis (ImageJ 1,48 v, National Institutes of Health, Bethesda, MD, USA) were performed relative to the internal control GAPDH.

XTT assay

To investigate whether 5-FU has any direct cytotoxic effect on effector cells and the NB cells NXS2-HGW that were used for tumor establishment *in vivo*, an *in vitro* XTT-based assay (Abcam, Germany) was performed according to the manufacturer's guidelines. Briefly, tumor cells were seeded into a 96-well plate at a density of 2.5×10^4 cells/well for 48 h followed by incubation with 5-FU (final concentrations: 5.6, 16.7, 50, 150, 450, and 1350 µg/ml) for 2 h. Thereafter, the cells were washed and incubated with the cell culture medium for 24 h. The rationale to incubate tumor cells with 5-FU for 2 h was based

Table 1. PCR conditions and primer sequences of CD11b+ myeloid cell-associated and modulating genes. To investigate mRNA expression of CD11b+ myeloid cell-associated and modulating genes in tumor tissue and the neuroblastoma cells NXS2-HGW, RT-PCR analysis was used.

Gene name	Primer sequences	Annealing temperature (°C)	Cycle number	Product size (bp)
GAPDH	FP: AACTTTGGCATTGTGGAAGG RP: ACACATTGGGGGTAGGAACA	55	22	223
Arg1	FP: ATCGGAGCGCCTTTCTCAAA RP: GCAGATTCCCAGAGCTGGTT	65	30	391
CCL2	FP: GAAGGAATGGGTCCAGACAT RP: ACGGGTCAACTTCACATTCA	62	28	127
IL-8	FP: CCATATCCACGGATGCGACA RP: AAGCCCGAAAGAGTCTCTGC	60	35	293
GM-CSF	FP: CTCACCCATCACTGTCACCC RP: TGAAATTGCCCCGTAGACCC	65	38	191
IDO	FP: CTGGGTCCTTGTGGCTAGAA RP: CAGGCCCAACTTCTCTGAGA	63	35	247
IL-1β	FP: TGCCACCTTTTGACAGTGATG RP: AAGGTCCACGGGAAAGACAC	61	33	220
IL-4	FP: CCATATCCACGGATGCGACA RP: AAGCCCGAAAGAGTCTCTGC	61	35	254
IL-6	FP: ACAAAGCCAGAGTCCTTCAGA RP: TGGTCCTTAGCCACTCCTTC	60	38	153
IL-6 r	FP: ACACACTGGTTCTGAGGGAC RP: CCCGTTGGTGGTGTTGATTT	60	40	239
IL-10	FP: TGGCCCAGAAATCAAGGAGC RP: CAGCAGACTCAATACACACT	62	35	264
INF-	FP: GCTCTGAGACAATGAACGCT RP: AAAGAGATAATCTGGCTCTGC	62	33	229
iNOS	FP: CCCCGCTACTACTCCATCAG RP: CCACTGACACTTCGCACAAA	64	33	185
M-CSF	FP: GGGCCTCCTGTTCTACAAGT RP: AGGGGTGGCTTTAGGGTACA	63	35	209
M-CSFr	FP: GAGGCTATGCTAGGACCCAG RP: AAGAAGTCGAGACAGGCCTC	66	27	160
TGF-β1	FP: TCAGACATTCGGGAAGCAGT RP: TCGAAAGCCCTGTATTCCGT	62	30	243
VEGF-A	FP: CACAGCAGATGTGAATGCAG RP: TTTACACGTCTGCGGATCTT	61	30	118

on the studies of pharmacokinetics of 5-FU showing a short half-life time (< 2 h) of this drug.[28] Applicated at 500 mg/m^2 in cancer patients, plasma levels of 5-FU decline rapidly (no longer detectable after 2 h following drug injection). Three hours prior to assessment, XTT solution was given to each sample and finally, absorbance of each sample was assessed at 450 nm. For analysis of 5-FU impact on effector cells (1×10^6 cells/well), fresh murine splenocytes were incubated for 2 h with 5-FU at the similar final concentrations as described for tumor cells and analyzed 24 h later by flow cytometry.

Statistics

For statistical analyses, Sigma Plot (Jandel Scientific Software, San Rafael, CA, USA) was used. First, the acquired data sets were tested for normal distribution and homogeneity of variance. On the basis of the outcome, a *t*-test was used to compare two normal distributed independent samples and analysis of variance (ANOVA) to compare more than two samples regarding the significance of a metric trait. For not normal distributed data sets, a Mann-Whitney *U* test and Kruskall-Wallis test were used for comparing two and more than two groups, respectively. For all *in vitro* analyses, at least three biological replicates, each of them including three technical replicates, were used and given as the arithmetic mean ± standard error of the mean (SEM). A P value of < 0.05 was considered significant (*), $P < .01$ very significant (**) and $P < .001$ extremely significant (***). A Kaplan Meier analysis was performed to visualize survival probabilities and compared using LogRank statistics (Mantel-Cox). For the evaluation of survival probabilities of treated mice, a tumor volume of at least 750 mm^3 (represents a critical tumor volume) and death ahead of schedule were defined as an event, respectively.

Acknowledgments

The authors thank Maria Asmus, Manuela Brüser and Theodor Koepp (University Medicine Greifswald, Pediatric Hematology and Oncology, Greifswald, Germany) for excellent technical assistance.

Disclosure statement

The authors report no conflict of interest.

Funding

This was provided by the University Medicine Greifswald and the Deutsche Forschungsgemeinschaft (DFG), Germany under Grant [SI-2147/1-2].

Abbreviations

5-FU	5-Fluorouracil
Ab	antibody
ADCC	antibody-dependent cellular cytotoxicity

CDC	complement-dependent cytotoxicity
EFS	event-free survival
GAPDH	glyceraldehyde 3-phosphate dehydrogenase
NB	neuroblastoma
OS	overall survival
T_{reg}	regulatory T cells
SEM	standard error of the mean

References

1. Whittle SB, Smith V, Doherty E, Zhao S, McCarty S, Zage PE. Overview and recent advances in the treatment of neuroblastoma. Expert Rev Anticancer Ther. 2017;17:369–386. doi:10.1080/14737140.2017.1285230.
2. Ladenstein R, Potschger U, Valteau-Couanet D, Luksch R, Castel V, Yaniv I, Laureys G, Brock P, Michon JM, Owens C, et al. Interleukin 2 with anti-GD2 antibody ch14.18/CHO (dinutuximab beta) in patients with high-risk neuroblastoma (HR-NBL1/SIOPEN): a multicentre, randomised, phase 3 trial. Lancet Oncol. 2018;19(12):1617–1629. doi:10.1016/S1470-2045(18)30578-3.
3. Zeng Y, Fest S, Kunert R, Katinger H, Pistoia V, Michon J, Lewis G, Ladenstein R, Lode HN. Anti-neuroblastoma effect of ch14.18 antibody produced in CHO cells is mediated by NK-cells in mice. Mol Immunol. 2005;42:1311–1319. doi:10.1016/j.molimm.2004.12.018.
4. Koehn TA, Trimble LL, Alderson KL, Erbe AK, McDowell KA, Grzywacz B, Hank JA, Sondel PM. Increasing the clinical efficacy of NK and antibody-mediated cancer immunotherapy: potential predictors of successful clinical outcome based on observations in high-risk neuroblastoma. Front Pharmacol. 2012;3:91. doi:10.3389/fphar.2012.00091.
5. Barker E, Mueller BM, Handgretinger R, Herter M, Yu AL, Reisfeld RA. Effect of a chimeric anti-ganglioside GD2 antibody on cell-mediated lysis of human neuroblastoma cells. Cancer Res. 1991;51:144–149.
6. Chen RL, Reynolds CP, Seeger RC. Neutrophils are cytotoxic and growth-inhibiting for neuroblastoma cells with an anti-GD2 antibody but, without cytotoxicity, can be growth-stimulating. Cancer Immunol Immunother. 2000;48:603–612. doi:10.1007/s002620050008.
7. Yu AL, Gilman AL, Ozkaynak MF, London WB, Kreissman SG, Chen HX, Smith M, Anderson B, Villablanca JG, Matthay KK, et al. Anti-GD2 antibody with GM-CSF, interleukin-2, and isotretinoin for neuroblastoma. N Engl J Med. 2010;363(14):1324–1334. doi:10.1056/NEJMoa0911123.
8. Siebert N, Zumpe M, Juttner M, Troschke-Meurer S, Lode HN. PD-1 blockade augments anti-neuroblastoma immune response induced by anti-GD2 antibody ch14.18/CHO. Oncoimmunology. 2017;6:e1343775. doi:10.1080/2162402X.2017.1343775.
9. Bianchi G, Vuerich M, Pellegatti P, Marimpietri D, Emionite L, Marigo I, Bronte V, Di Virgilio F, Pistoia V, Raffaghello L, et al. ATP/P2X7 axis modulates myeloid-derived suppressor cell functions in neuroblastoma microenvironment. Cell Death Dis. 2014;5:e1135. doi:10.1038/cddis.2014.109.
10. Carlson LM, Rasmuson A, Idborg H, Segerstrom L, Jakobsson PJ, Sveinbjornsson B, Kogner P. Low-dose aspirin delays an inflammatory tumor progression in vivo in a transgenic mouse model of neuroblastoma. Carcinogenesis. 2013;34:1081–1088. doi:10.1093/carcin/bgt009.
11. Dierckx de Casterlé I, Fevery S, Rutgeerts O, Poosti F, Struyf S, Lenaerts C, Waer M, Billiau AD, Sprangers B, Dierckx de Casterle I, Fevery S, Rutgeerts O, Poosti F, Struyf S, Lenaerts C. Reduction of myeloid-derived suppressor cells reinforces the anti-solid tumor effect of recipient leukocyte infusion in murine neuroblastoma-bearing allogeneic bone marrow chimeras. Cancer Immunol Immunother. 2018;67:589–603. doi:10.1007/s00262-017-2114-8.
12. Kroesen M, Bull C, Gielen PR, Brok IC, Armandari I, Wassink M, Looman MWG, Boon L, den Brok MH, Hoogerbrugge PM, et al. Anti-GD2 mAb and Vorinostat synergize in the treatment of neuroblastoma. Oncoimmunology. 2016;5:e1164919. doi:10.1080/2162402X.2016.1164919.
13. Asgharzadeh S, Salo JA, Ji L, Oberthuer A, Fischer M, Berthold F, Hadjidaniel M, Liu CWY, Metelitsa LS, Pique-Regi R, et al. Clinical significance of tumor-associated inflammatory cells in metastatic neuroblastoma. J clini oncol. 2012;30:3525–3532. doi:10.1200/JCO.2011.40.9169.
14. Santilli G, Piotrowska I, Cantilena S, Chayka O, D'Alicarnasso M, Morgenstern DA, Himoudi N, Pearson K, Anderson J, Thrasher AJ, et al. Polyphenon [corrected] E enhances the anti-tumor immune response in neuroblastoma by inactivating myeloid suppressor cells. Clini Cancer Res. 2013;19:1116–1125. doi:10.1158/1078-0432.CCR-12-2528.
15. Vincent J, Mignot G, Chalmin F, Ladoire S, Bruchard M, Chevriaux A, Martin F, Apetoh L, Rebe C, Ghiringhelli F, et al. 5-Fluorouracil selectively kills tumor-associated myeloid-derived suppressor cells resulting in enhanced T cell-dependent antitumor immunity. Cancer Res. 2010;70(8):3052–3061. doi:10.1158/0008-5472.CAN-09-3690.
16. Keyel ME, Reynolds CP. Spotlight on dinutuximab in the treatment of high-risk neuroblastoma: development and place in therapy. Biologics. 2019;13:1–12.
17. Vetsika EK, Koukos A, Myeloid-Derived Suppressor KA. Cells: major figures that shape the immunosuppressive and angiogenic network in cancer. Cells. 2019;8:1647. doi:10.3390/cells8121647.
18. Abiko K, Matsumura N, Hamanishi J, Horikawa N, Murakami R, Yamaguchi K, Yoshioka Y, Baba T, Konishi I, Mandai M, et al. IFN-gamma from lymphocytes induces PD-L1 expression and promotes progression of ovarian cancer. Br J Cancer. 2015;112:1501–1509. doi:10.1038/bjc.2015.101.
19. Spranger S, Spaapen RM, Zha Y, Williams J, Meng Y, Ha TT, Gajewski TF. Up-regulation of PD-L1, IDO, and T(regs) in the melanoma tumor microenvironment is driven by CD8(+) T cells. Sci Transl Med. 2013;5:200ra116. doi:10.1126/scitranslmed.3006504.
20. Mo X, Zhang H, Preston S, Martin K, Zhou B, Vadalia N, Gamero AM, Soboloff J, Tempera I, Zaidi MR, et al. Interferon-gamma signaling in melanocytes and melanoma cells regulates expression of CTLA-4. Cancer Res. 2018;78:436–450. doi:10.1158/0008-5472.CAN-17-1615.
21. Ostrand-Rosenberg S, Sinha P. Myeloid-derived suppressor cells: linking inflammation and cancer. J Immunol. 2009;182(8):4499–4506. doi:10.4049/jimmunol.0802740.
22. Lode HN, Schmidt M, Seidel D, Huebener N, Brackrock D, Bleeke M, Reker D, Brandt S, Mueller H-P, Helm C, et al. Vaccination with anti-idiotyp e antibody ganglidiomab mediates a GD(2)-specific anti-neuroblastoma immune response. Cancer Immunol Immunother. 2013;62:999–1010. doi:10.1007/s00262-013-1413-y.
23. Lode HN, Xiang R, Varki NM, Dolman CS, Gillies SD, Reisfeld RA. Targeted interleukin-2 therapy for spontaneous neuroblastoma metastases to bone marrow. J Natl Cancer Inst. 1997;89:1586–1594. doi:10.1093/jnci/89.21.1586.
24. Kawane K, Tanaka H, Kitahara Y, Shimaoka S, Nagata S. Cytokine-dependent but acquired immunity-independent arthritis caused by DNA escaped from degradation. Proc Natl Acad Sci USA. 2010;107(45):19432–19437.doi: 10.1073/pnas.1010603107.
25. McCarthy MK, Procario MC, Twisselmann N, Wilkinson JE, Archambeau AJ, Michele DE, Day SM, Weinberg JB. Proinflammatory effects of interferon gamma in mouse adenovirus 1 myocarditis. J Virol. 2015;89:468–479.
26. Schiller KR, Zillhardt MR, Alley J, Borjesson DL, Beitz AJ, Mauro LJ. Secretion of MCP-1 and other paracrine factors in a novel tumor-bone coculture model. BMC Cancer. 2009;9:45. doi:10.1186/1471-2407-9-45.
27. Woo YD, Koh J, Kang H-R, Kim HY, Chung DH. The invariant natural killer T cell–mediated chemokine X-C motif chemokine ligand 1–X-C motif chemokine receptor 1 axis promotes allergic airway hyperresponsiveness by recruiting CD103+ dendritic cells. J Allergy Clini Immunol. 2018;142:1781–92.e12. doi:10.1016/j.jaci.2017.12.1005.
28. Heggie GD, Sommadossi JP, Cross DS, Huster WJ, Diasio RB. Clinical pharmacokinetics of 5-fluorouracil and its metabolites in plasma, urine, and bile. Cancer Res. 1987;47:2203–2206.